




## Article

# Impact of Dexamethasone on Three-Dimensional Stem Cell Spheroids: Morphology, Viability, Osteogenic Differentiation

Heera Lee <sup>1,2,†</sup> , Ju-Hwan Kim <sup>1,†</sup>, Hyun-Jin Lee <sup>1</sup>  and Jun-Beom Park <sup>1,2,3,\*</sup> 

<sup>1</sup> Department of Periodontics, College of Medicine, The Catholic University of Korea, Seoul 06591, Republic of Korea; yysmj@naver.com (H.L.); juhwank33@naver.com (J.-H.K.); hyunjinlee0423@gmail.com (H.-J.L.)

<sup>2</sup> Department of Medicine, Graduate School, The Catholic University of Korea, Seoul 06591, Republic of Korea

<sup>3</sup> Dental Implantology, Graduate School of Clinical Dental Science, The Catholic University of Korea, Seoul 06591, Republic of Korea

\* Correspondence: jbasoon@catholic.ac.kr; Tel.: +82-2-2258-6290

† These authors contributed equally to this work.

**Abstract:** *Background and Objectives:* Dexamethasone has been widely researched for its ability to promote osteogenic differentiation in mesenchymal stem cells in basic research. This study focused on examining the effects of dexamethasone on both cell viability and osteogenic differentiation in three-dimensional stem cell spheroids. *Materials and Methods:* These spheroids were created using concave microwells and exposed to dexamethasone at concentrations ranging from 0  $\mu$ M to 100  $\mu$ M, including intermediate levels of 0.1  $\mu$ M, 1  $\mu$ M, and 10  $\mu$ M. Microscopic analysis was used to qualitatively assess cellular viability, while a water-soluble tetrazolium salt-based assay provided quantitative viability data. Osteogenic differentiation was evaluated by measuring alkaline phosphatase activity and calcium deposition using Alizarin Red staining. Additionally, the expression levels of genes associated with osteogenesis were measured through quantitative polymerase chain reaction. *Results:* The spheroids successfully self-assembled within the first 24 h and maintained their structural integrity over a seven-day period. Analysis of cell viability showed no statistically significant differences across the various dexamethasone concentrations tested. Although there was an observed increase in alkaline phosphatase activity and calcium deposition following dexamethasone treatment, these differences were not statistically significant. RUNX2 gene expression was upregulated in the 1  $\mu$ M, 10  $\mu$ M, and 100  $\mu$ M groups, while COL1A1 expression significantly increased at 0.1  $\mu$ M and 1  $\mu$ M. *Conclusions:* These results indicate that dexamethasone supports cell viability and enhances RUNX2 and COL1A1 expression in stem cell spheroids.

**Keywords:** cell survival; cell differentiation; cellular spheroids; dexamethasone; osteogenesis; stem cells



Academic Editors: Vita Maciulskiene and Gaetano Isola

Received: 12 April 2025

Revised: 29 April 2025

Accepted: 6 May 2025

Published: 9 May 2025

**Citation:** Lee, H.; Kim, J.-H.; Lee, H.-J.; Park, J.-B. Impact of Dexamethasone on Three-Dimensional Stem Cell Spheroids: Morphology, Viability, Osteogenic Differentiation. *Medicina* **2025**, *61*, 871. <https://doi.org/10.3390/medicina61050871>

**Copyright:** © 2025 by the authors. Published by MDPI on behalf of the Lithuanian University of Health Sciences. Licensee MDPI, Basel, Switzerland. This article is an open access article distributed under the terms and conditions of the Creative Commons Attribution (CC BY) license (<https://creativecommons.org/licenses/by/4.0/>).

## 1. Introduction

Dexamethasone, a synthetic glucocorticoid, is commonly used in stem cell research for its potent anti-inflammatory and immunosuppressant properties [1,2]. Dexamethasone can influence various aspects of the behavior and the differentiation of stem cells [3]. In tissue engineering, dexamethasone is often used to enhance the formation of bone and cartilage tissues [4]. Dexamethasone promotes the synthesis of extracellular matrix components, including collagen type I and bone sialoprotein, during the process of osteogenesis [5]. Dexamethasone influences the expression of genes associated with osteogenic differentiation, including RUNX2 and SOX9 [4,6].

Stem cells have recently garnered significant attention, particularly in research and the medical field [7–9]. They are a type of undifferentiated cell capable of both self-renewal and differentiation into specialized cell types [7]. Owing to these abilities, stem cells have attracted considerable interest for their potential to repair injured tissues and treat a range of diseases [10]. They are commonly classified based on their capacity for self-renewal, differentiation, and their source. Adult stem cells, such as mesenchymal stem cells (MSCs), exhibit multipotency, allowing them to differentiate into various cell types of their tissue of origin [11]. Conversely, induced pluripotent stem cells are adult cells that have been genetically reprogrammed to exhibit pluripotency, enabling differentiation into any cell type in the body [12]. Stem cells possess the capability to replenish or restore damaged tissues and organs [13]. Additionally, they can be applied to develop models for drug testing or disease modeling [9,14,15]. A three-dimensional stem cell-based model enables an efficient and reproducible formation of spheroids, which maintain structural integrity over several weeks and demonstrate enhanced osteogenic differentiation compared to conventional two-dimensional cultures [16]. The combination of stem cells with molecules such as growth factors has been reported to enhance bone regeneration and angiogenesis [17,18]. To undergo vigorous osteogenic development *in vitro*, mesenchymal stem cells require additional agonists [19,20]. The use of dexamethasone on MSCs has also been shown to regulate immune responses by influencing interactions between MSCs and immune cells [21]. Specifically, dexamethasone-treated MSCs can suppress immune cell proliferation and modulate the behavior of T cells and macrophages [22,23].

Dexamethasone, a synthetic glucocorticoid, is widely recognized for promoting osteogenic differentiation by regulating key transcription factors such as RUNX2 and enhancing the production of extracellular matrix proteins, including type I collagen. In conventional two-dimensional (2D) cultures, dexamethasone has been shown to induce osteoblast differentiation and matrix mineralization. However, its effects within three-dimensional (3D) spheroid systems, particularly those formed from gingiva-derived mesenchymal stem cells (GMSCs), remain insufficiently characterized.

Given that 3D spheroid models more closely replicate the native cellular microenvironment and promote enhanced cell–cell and cell–matrix interactions, evaluating the impact of dexamethasone in this context is essential for optimizing stem cell-based regenerative therapies. Therefore, the present study aimed to investigate the effects of dexamethasone on the cellular morphology, viability, osteogenic potential, and gene expression of GMSC spheroids, providing novel insights into its potential applications in bone tissue engineering and regenerative medicine.

## 2. Materials and Methods

### 2.1. Generation of Cell Spheroids Using Gingiva-Derived Mesenchymal Stem Cells

The Institutional Review Board at Seoul St. Mary's Hospital, College of Medicine, The Catholic University of Korea, granted approval for the research protocol (KC22SISI0513) on 22 August 2022. Mesenchymal stem cells were extracted from gingival tissue and processed using established methods for isolation and characterization [24]. Following initial seeding on culture dishes, cells that did not adhere were removed, and the culture medium was refreshed every two to three days. For the creation of spheroids, commercially available concave microwells (H389600, StemFIT 3D; MicroFIT, Seongnam-si, Gyeonggi-do, Republic of Korea) were used. Each microwell was populated with one million stem cells, facilitating spheroid formation through cell-to-cell adhesion. To assess its effect on spheroid development, dexamethasone was applied in concentrations ranging from 0  $\mu$ M to 100  $\mu$ M, including intermediate levels of 0.1  $\mu$ M, 1  $\mu$ M, and 10  $\mu$ M. The morphological characteristics of the spheroids were observed and evaluated on Days 1, 3, 5, and 7.

## 2.2. The Assessment of Cellular Viability

Stem cell spheroids were cultured in osteogenic media, with evaluations conducted at predetermined intervals. Qualitative assessments of the spheroids were carried out on Days 1 and 3 using a dual-color assay designed to detect plasma membrane integrity and esterase activity, utilizing propidium iodide and calcein acetoxymethyl ester (Live/Dead Kit assay, Molecular Probes, Eugene, OR, USA) [25]. Furthermore, quantitative analysis of cellular viability was performed on Days 1, 3, 5, and 7 using a water-soluble tetrazolium salt-based assay (Cell Counting Kit-8, Dojindo, Tokyo, Japan) [26]. For each condition and time point, three technical replicates were evaluated.

## 2.3. Quantification of Alkaline Phosphatase Activity and Calcium Deposition

Osteogenic differentiation was evaluated by measuring alkaline phosphatase (ALP) activity and quantifying calcium deposition using an anthraquinone dye-based method [27]. Stem cell spheroids cultured under osteogenic conditions were collected on Days 7 and 14. ALP activity was assessed using a commercially available assay kit (K412-500, BioVision, Inc., Milpitas, CA, USA). Calcium deposition analysis was conducted on Days 7 and 14 employing an anthraquinone dye assay [28]. Prior to staining, the spheroids underwent sequential washing and fixation. Alizarin Red S staining was subsequently applied at room temperature for 30 min. Following the staining procedure, the bound dye was extracted, and its concentration was determined using cetylpyridinium chloride.

## 2.4. Total RNA Extraction and Real-Time Polymerase Chain Reaction Quantification

RNA was extracted to assess its yield and integrity. The concentration of RNA was determined through spectrophotometric analysis (ND-2000, Thermo Fisher Scientific, Inc., Waltham, MA, USA) by measuring absorbance at 260 nm and 280 nm. To quantify mRNA expression levels, real-time quantitative polymerase chain reaction (qPCR) was conducted [29]. The primer sequences employed in this study are provided in Table 1.  $\beta$ -actin was utilized as an internal reference for normalization.

**Table 1.** The primer sequences used for real-time quantitative polymerase chain reaction (qPCR).

Gene	Forward Primer (5' → 3')	Reverse Primer (5' → 3')
RUNX2	AAGTGCGGTGCAAACTTTCT	TCTCGGTGGCTGCTAGTGA
COL1A1	CCAGAAGAACTGGTACATCAGCAA	TGGTTTCTTCTCCTCTGCGC
$\beta$ -actin	TGGCACCCAG CACAATGAA	CTAAGTCATAGTCCGCCTAGAAGCA

## 2.5. Statistical Analysis

Statistical data were presented as mean values with corresponding standard deviations for each experimental group. To ensure the validity of statistical assumptions, assessments of normality and homogeneity of variance were conducted to verify that the dataset conformed to a normal distribution and exhibited consistent variance. The experimental results, influenced by dexamethasone concentration and time points, were analyzed using a two-way ANOVA. Furthermore, groupwise comparisons were performed using a one-way ANOVA, followed by Tukey's post hoc test, with all calculations executed using SPSS 12 (SPSS Inc., Chicago, IL, USA). A significance level was established at  $p < 0.05$ .

# 3. Results

## 3.1. Generation of Spheroid-Shaped Stem Cell Aggregates

Figure 1A illustrates the morphological alterations observed in spheroids subjected to dexamethasone treatment at concentrations ranging from 0  $\mu$ M to 100  $\mu$ M, including

intermediate concentrations of 0.1  $\mu\text{M}$ , 1  $\mu\text{M}$ , and 10  $\mu\text{M}$ , over a period of Days 1, 3, 5, and 7. Throughout this seven-day observation period, the spheroids maintained their overall structural integrity, with no significant morphological deviations detected. Although minor variations in spheroid size were noted between Day 1 and Day 7, the characteristic rounded shape of the spheroids was consistently preserved. The diameters of the spheroids measured on Days 1, 3, 5, and 7 are summarized in Figure 1B. On Day 1, the recorded spheroid diameters for each dexamethasone concentration were as follows:  $217.9 \pm 25.4 \mu\text{m}$  (control, 0  $\mu\text{M}$ ),  $218.2 \pm 9.1 \mu\text{m}$  (0.1  $\mu\text{M}$ ),  $193.3 \pm 15.5 \mu\text{m}$  (1  $\mu\text{M}$ ),  $219.4 \pm 22.4 \mu\text{m}$  (10  $\mu\text{M}$ ), and  $232.1 \pm 7.5 \mu\text{m}$  (100  $\mu\text{M}$ ). No statistically significant differences were observed among the groups at this time point ( $p > 0.05$ ). Similarly, spheroid diameters on Day 3 showed no significant variations across treatment conditions ( $p > 0.05$ ). However, a statistically significant increase in spheroid size was observed in the 100  $\mu\text{M}$  group on Days 5 and 7 ( $p < 0.05$ ).

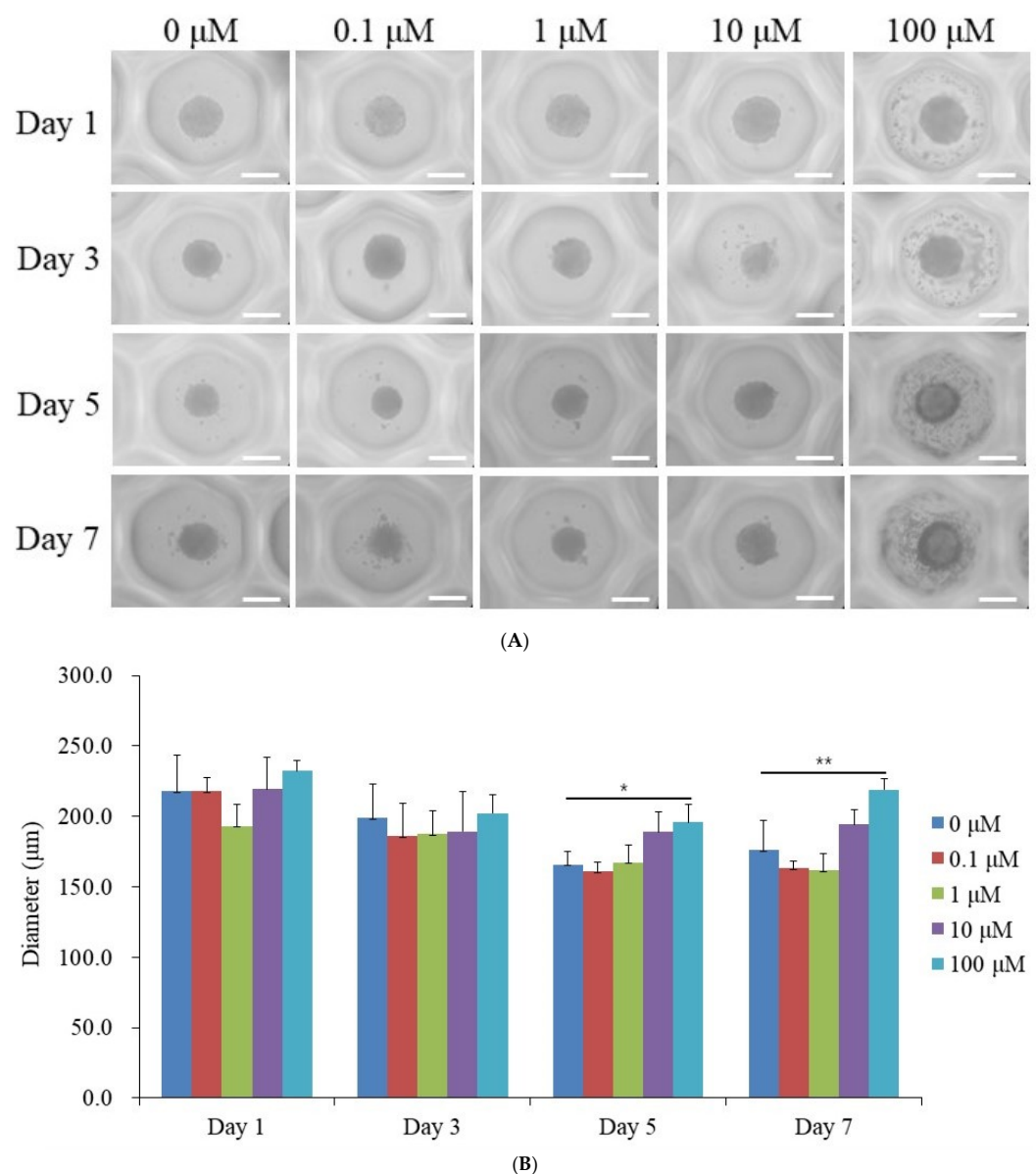


**Figure 1.** Morphological evaluation. (A) The morphology of the stem-cell spheroids at Days 1, 3, 5, and 7. The provided scale bar represents a length of 200  $\mu\text{m}$ . (B) The diameter of the stem cell spheroids on Days 1, 3, 5, and 7. \*  $p < 0.05$  compared to the 0  $\mu\text{M}$  group on Day 5. \*\*  $p < 0.05$  compared to the 0  $\mu\text{M}$  group on Day 7.

### 3.2. Assessment of Cell Viability

Figure 2A,B present a qualitative evaluation of stem cell viability on Days 1 and 3, utilizing the Live/Dead Kit assay. As depicted in Figure 2A, the majority of stem cells displayed a rounded morphology with pronounced green fluorescence on Day 3, indicative of their viability. Similarly, Figure 2B demonstrates sustained green fluorescence following extended incubation, confirming stable cell survival through Day 3. A quantitative analysis of cell viability across multiple time points (Days 1, 3, 5, and 7) is illustrated in Figure 2C. As shown in Figure 2C, cell viability, as assessed by absorbance at 450 nm, remained consistently high across all dexamethasone concentrations. On Day 1, the 0.1  $\mu\text{M}$  group demonstrated the highest absorbance ( $0.399 \pm 0.008$ ), followed by the 10  $\mu\text{M}$  ( $0.391 \pm 0.025$ ), 1  $\mu\text{M}$  ( $0.372 \pm 0.052$ ), and 100  $\mu\text{M}$  ( $0.375 \pm 0.033$ ) groups, whereas the control exhibited the lowest value ( $0.302 \pm 0.066$ ). Similar trends were observed on Day 3, with the 0.1  $\mu\text{M}$  group maintaining the highest viability ( $0.410 \pm 0.040$ ) and the control group showing the lowest ( $0.311 \pm 0.045$ ). No significant differences were observed among the groups ( $p > 0.05$ ).

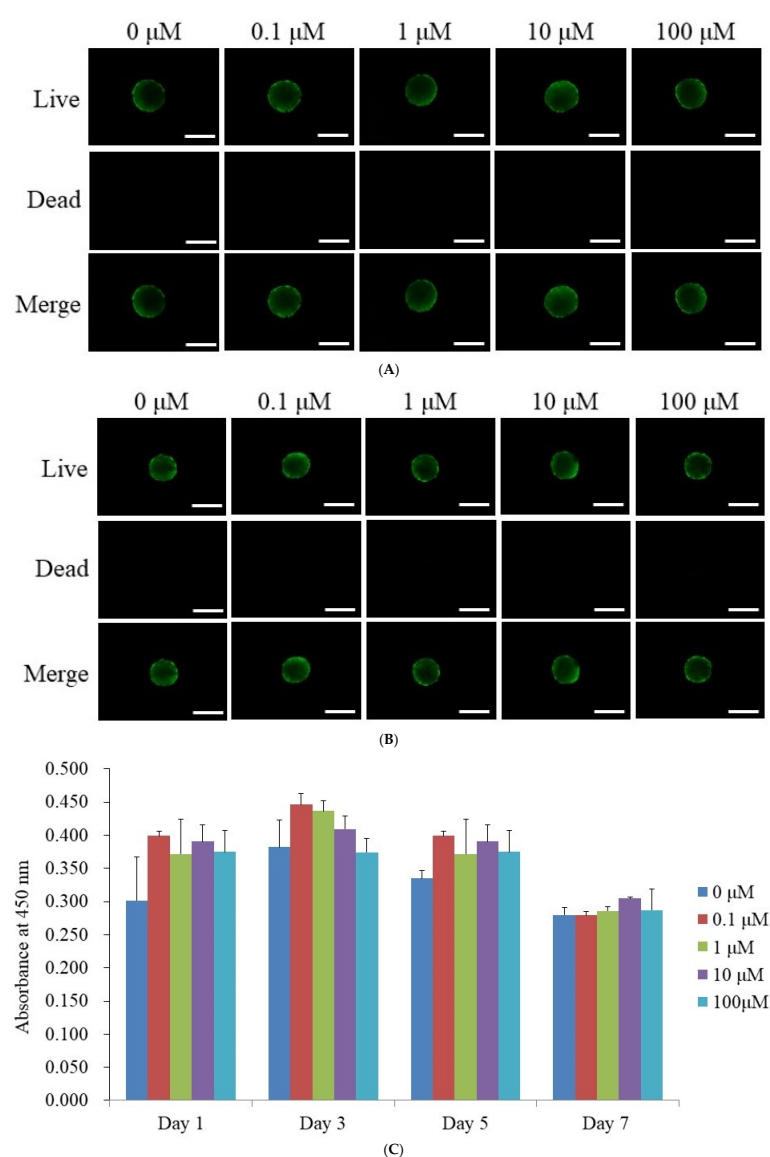


**Figure 2.** Composite images illustrating the viability of stem cell spheroids. (A) Representative merged images depicting live and dead cells within spheroids on Day 1, with a scale bar of 200  $\mu\text{m}$ . (B) Composite visualization of live, dead, and merged spheroid images captured on Day 3. (C) Quantitative assessment of cellular viability conducted using the CCK-8 assay on Days 1, 3, 5, and 7.

### 3.3. Alkaline Phosphatase Activity Levels and Calcium Deposition Extent

The findings of the ALP activity assay performed on Days 7 and 14 are summarized in Figure 3A. Absorbance measurements taken at 405 nm on Day 7 were recorded as follows:  $0.352 \pm 0.004$  for the control (0  $\mu\text{M}$ ),  $0.352 \pm 0.024$  for 0.1  $\mu\text{M}$ ,  $0.372 \pm 0.011$  for 1  $\mu\text{M}$ ,  $0.376 \pm 0.009$  for 10  $\mu\text{M}$ , and  $0.371 \pm 0.013$  for 100  $\mu\text{M}$ . While the average absorbance values in the 1  $\mu\text{M}$ , 10  $\mu\text{M}$ , and 100  $\mu\text{M}$  groups were slightly elevated compared to the control, these differences were not statistically significant ( $p > 0.05$ ). Similarly, ALP activity on Day 14 did not show a significant deviation from the untreated control group.

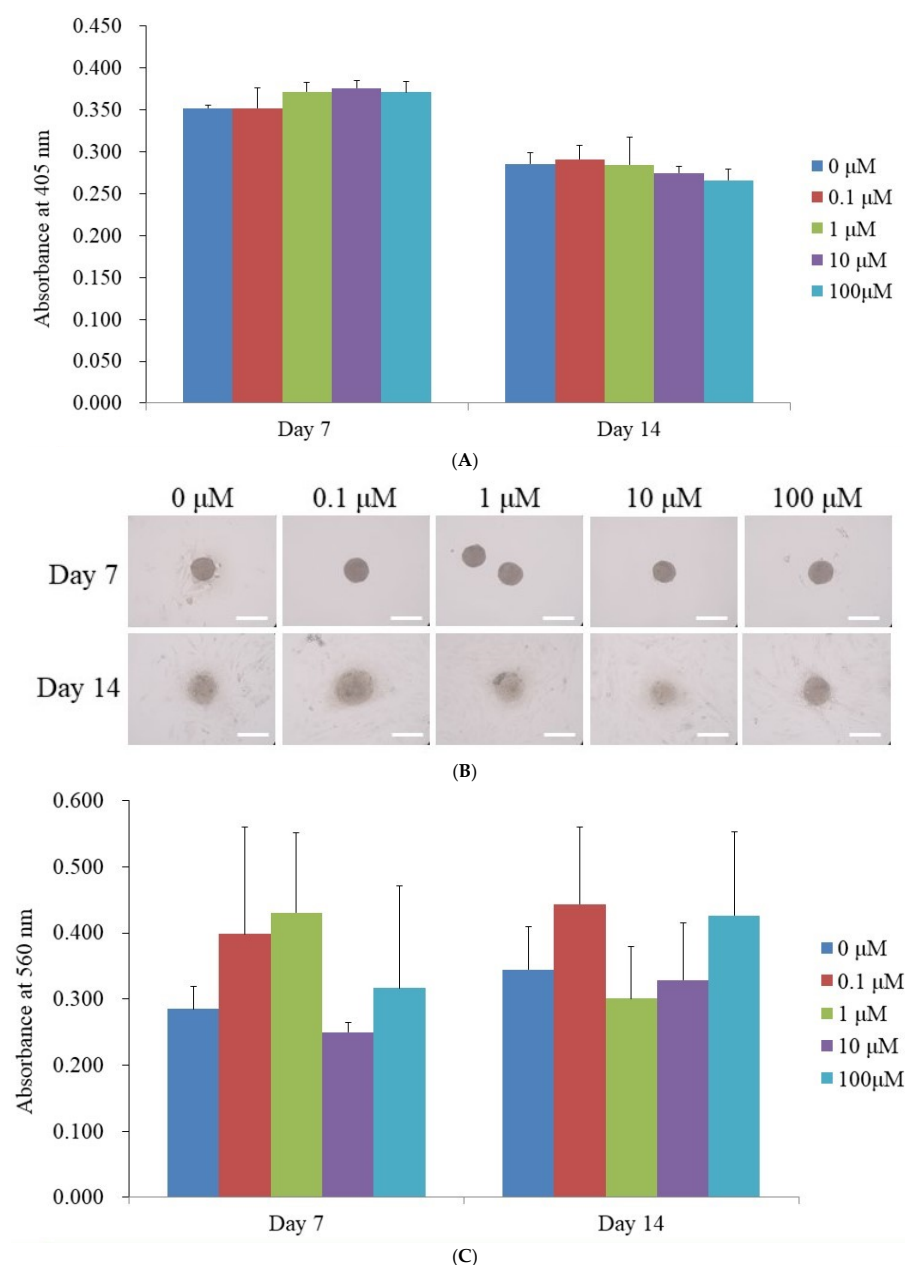


**Figure 3.** Osteogenic maturation of stem cell spheroids. (A) Alkaline phosphatase activity levels on Days 7 and 14. (B) Microscopic visualization of Alizarin Red S staining results on Days 7 and 14, with a scale bar of 200  $\mu\text{m}$ . (C) Quantitative analysis of Alizarin Red S staining.

Distinct calcium deposits were visible in all groups at both time points, as depicted in Figure 3B. The relative calcium deposition levels measured on Day 7 were  $0.285 \pm 0.034$  (0  $\mu\text{M}$ ),  $0.399 \pm 0.161$  (0.1  $\mu\text{M}$ ),  $0.431 \pm 0.121$  (1  $\mu\text{M}$ ),  $0.250 \pm 0.014$  (10  $\mu\text{M}$ ), and  $0.316 \pm 0.155$  (100  $\mu\text{M}$ ), as illustrated in Figure 3C. On Day 14, the corresponding cal-



cium deposition values were  $0.345 \pm 0.065$  for 0  $\mu\text{M}$ ,  $0.444 \pm 0.116$  for 0.1  $\mu\text{M}$ ,  $0.301 \pm 0.078$  for 1  $\mu\text{M}$ ,  $0.329 \pm 0.086$  for 10  $\mu\text{M}$ , and  $0.427 \pm 0.127$  for 100  $\mu\text{M}$ .

### 3.4. Evaluation of RUNX2 and COL1A1 Quantitative Real-Time Polymerase Chain Reaction

qPCR analysis was performed to quantify the mRNA expression levels of RUNX2 and COL1A1 on Days 7 and 14. The mRNA expression of RUNX2 measured on Day 7 exhibited the following values for each dexamethasone concentration:  $1.000 \pm 0.915$  (0  $\mu\text{M}$ , control),  $13.007 \pm 10.423$  (0.1  $\mu\text{M}$ ),  $3.152 \pm 3.054$  (1  $\mu\text{M}$ ),  $7.440 \pm 4.436$  (10  $\mu\text{M}$ ), and  $4.875 \pm 3.973$  (100  $\mu\text{M}$ ). No statistically significant differences were observed among the groups ( $p > 0.05$ ) (Figure 4A). On Day 14, an upward trend in RUNX2 mRNA levels was observed, with values recorded as  $2.830 \pm 2.843$  (0  $\mu\text{M}$ ),  $9.544 \pm 3.408$  (0.1  $\mu\text{M}$ ),  $9.851 \pm 1.138$  (1  $\mu\text{M}$ ),  $13.535 \pm 2.311$  (10  $\mu\text{M}$ ), and  $16.710 \pm 4.937$  (100  $\mu\text{M}$ ), demonstrating statistical significance ( $p < 0.05$ ). Similarly, the mRNA expression of COL1A1 on Day 7 was quantified as  $1.000 \pm 0.025$  (0  $\mu\text{M}$ , control),  $4.531 \pm 0.197$  (0.1  $\mu\text{M}$ ),  $1.268 \pm 0.025$  (1  $\mu\text{M}$ ),  $1.122 \pm 0.016$  (10  $\mu\text{M}$ ), and  $0.561 \pm 0.029$  (100  $\mu\text{M}$ ), showing a significant increase compared to the control ( $p < 0.05$ ) (Figure 4B). By Day 14, COL1A1 expression continued to rise, with measured values of  $1.355 \pm 0.148$  (0  $\mu\text{M}$ , control),  $1.497 \pm 0.199$  (0.1  $\mu\text{M}$ ),  $1.804 \pm 0.157$  (1  $\mu\text{M}$ ),  $1.335 \pm 0.070$  (10  $\mu\text{M}$ ), and  $0.575 \pm 0.048$  (100  $\mu\text{M}$ ), confirming statistical significance ( $p < 0.05$ ).

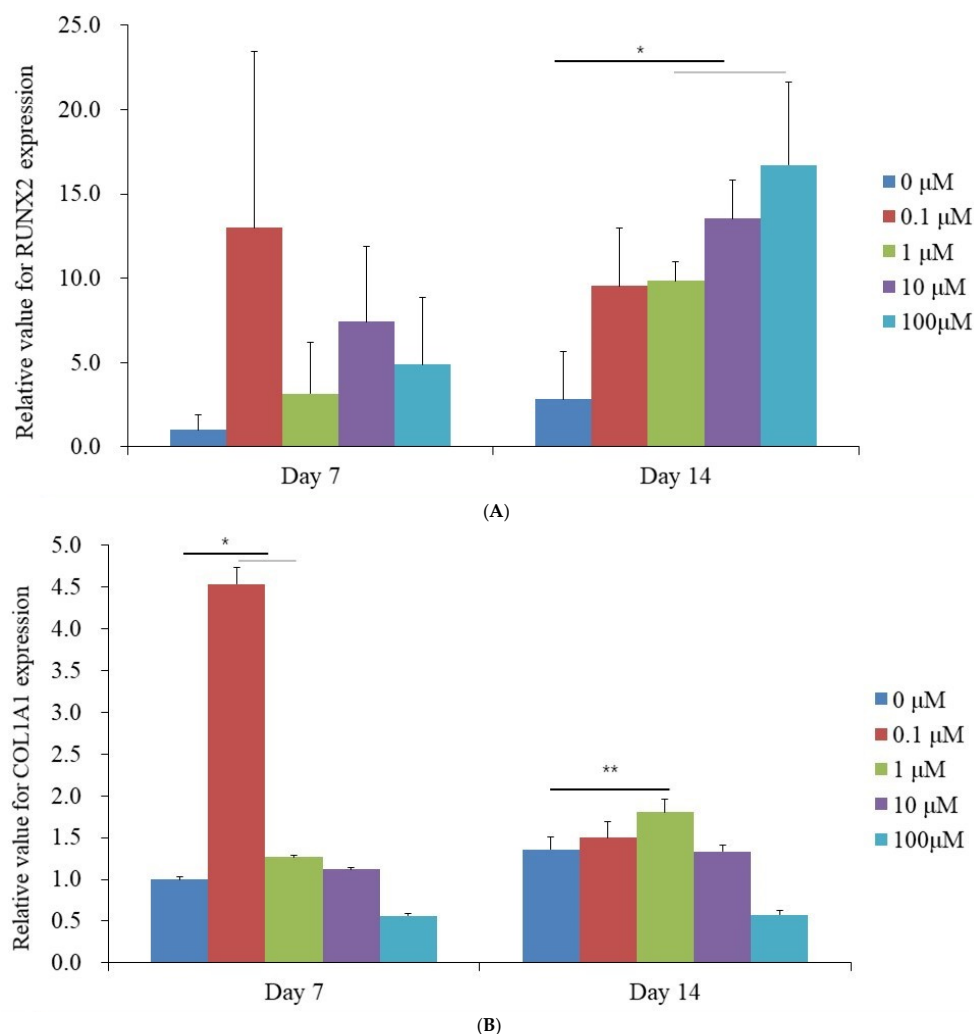


**Figure 4.** Quantification by real-time polymerase chain reaction on Days 7 and 14. **(A)** Expression of RUNX2. \*  $p < 0.05$  compared to the 0  $\mu\text{M}$  group on Day 14. **(B)** Expression of COL1A1. \*  $p < 0.05$  compared to the 0  $\mu\text{M}$  group on Day 7. \*\*  $p < 0.05$  compared to the 0  $\mu\text{M}$  group on Day 14.

#### 4. Discussion

This study examined the impact of dexamethasone on the structural integrity, cellular viability, and osteogenic differentiation of stem cell spheroids. These findings extend previous research that has extensively investigated dexamethasone's role in modulating mesenchymal stem cell behavior and differentiation under various experimental conditions. The concentration of dexamethasone used in prior studies varied significantly based on the experimental design. This report demonstrated that morphological stability was maintained throughout the tested period. For instance, rat bone marrow-derived and muscle tissue-derived stem cells cultured in media with or without 10  $\mu\text{M}$  dexamethasone demonstrated their efficacy in promoting osteogenesis [30]. Other studies employed dexamethasone at 1 and 100 nM for chondrogenesis [31], while higher concentrations, such as 1  $\mu\text{M}$ , were shown to negatively impact cell activity by promoting apoptosis, increasing oxidative stress, and disrupting mitochondrial dynamics [32]. Additionally, studies examining concentrations between 2.55  $\mu\text{M}$  and 7.64  $\mu\text{M}$  over 24–48 h found that dexamethasone preserved mesenchymal stem cell morphology and viability without inducing cytotoxicity [3]. These findings collectively underscore the necessity for dose optimization to achieve therapeutic benefits without adverse effects. In this study, dexamethasone concentrations of 0.1  $\mu\text{M}$ , 1  $\mu\text{M}$ , 10  $\mu\text{M}$ , and 100  $\mu\text{M}$  did not significantly impact the viability of stem cells cultured in three-dimensional spheroid models. This observation highlights the potential of spheroid culture systems to mimic *in vivo* environments, possibly enhancing cellular resilience against stress. In another report, the effects of various dexamethasone concentrations, ranging from 50 nM to 10  $\mu\text{M}$ , showed that dexamethasone influenced spheroid formation in a concentration-dependent manner, with higher concentrations disrupting aggregation and leading to the disassembly of cell aggregates in culture dishes [33]. Furthermore, RUNX2 expression was upregulated at 1  $\mu\text{M}$ , 10  $\mu\text{M}$ , and 100  $\mu\text{M}$ , while COL1A1 expression was significantly upregulated at 0.1  $\mu\text{M}$  and 1  $\mu\text{M}$ . These concentrations appeared to improve the functional properties of the spheroids, consistent with dexamethasone's known role in promoting osteogenesis. Calcium deposition, visualized and quantified through Alizarin Red S staining, represents late-stage osteogenic maturation, corresponding to the mineralization phase of bone tissue development. The increased calcium accumulation, although not statistically significant across groups, suggests that dexamethasone may promote matrix mineralization in 3D GMSC spheroids, which is crucial for the mechanical strength and functional integrity of regenerated bone.

The evaluation of ALP activity, a crucial indicator of osteogenic differentiation, confirmed that dexamethasone promotes early-stage bone formation [34]. ALP is prominently expressed during osteoblast differentiation and serves as a fundamental measure for assessing osteogenic potential *in vitro* [27]. The increased ALP activity observed in this study is consistent with previous findings, reinforcing dexamethasone's capacity to initiate osteogenesis and its potential application in bone tissue engineering [35,36]. The analysis of mRNA expression for RUNX2 and COL1A1 provided further insights into the molecular mechanisms underlying dexamethasone-induced osteogenesis. RUNX2, a pivotal transcription factor, regulates osteoblast differentiation and skeletal growth by activating downstream genes [37]. COL1A1 encodes type I collagen, a vital structural component of the bone matrix that contributes to its mechanical strength and quality [38]. The elevated expression of COL1A1 suggests that dexamethasone may enhance the structural integrity of newly formed bone, thereby accelerating recovery and improving therapeutic outcomes. The significant upregulation of RUNX2 and COL1A1 observed in this study indicates that dexamethasone enhances the transcriptional network essential for bone formation [39]. Previous studies have demonstrated that stem cell spheroids can promote functional bone regeneration *in vivo* by enhancing osteogenic differentiation and vascularization [40,41],



supporting the potential translational application of GMSC spheroids treated with dexamethasone for bone tissue engineering and regenerative therapies. These findings highlight the clinical significance of dexamethasone treatment, suggesting its potential to improve outcomes in bone grafting, dental implants, and fracture healing. Its dose-dependent effects present opportunities for personalized therapeutic strategies tailored to patient-specific needs, such as severe bony defects or delayed healing. Furthermore, combining dexamethasone with osteoinductive agents like bone morphogenetic proteins or vascular endothelial growth factors could enhance its therapeutic efficacy by simultaneously promoting osteogenesis and angiogenesis.

Despite these promising results, several limitations inherent in this study must be acknowledged. Three-dimensional stem cell spheroids exhibit considerable potential for diverse tissue engineering applications; however, current spheroid fabrication methods face challenges such as diminished cell viability due to limited oxygen availability at the core and nonspecific differentiation resulting from the complex post-transplantation environment [42]. Additionally, the administration of dexamethasone may impede spheroid formation, necessitating careful regulation of its application timing [43].

As this investigation was conducted entirely *in vitro*, the findings require *in vivo* validation to ascertain the long-term effects of dexamethasone on bone regeneration and remodeling. Furthermore, while this study concentrated on RUNX2 and COL1A1 as primary markers, future research should encompass a broader spectrum of osteogenic markers, including osteocalcin, osteopontin, and bone sialoprotein, to achieve a more comprehensive understanding of dexamethasone's impact on osteogenesis [44].

Bone formation is intricately modulated by the interaction between osteogenesis and angiogenesis, and the potential for multidirectional cell differentiation in stem cell-based spheroids may offer promising future applications [45]. Future investigations should explore the synergistic potential of dexamethasone with advanced tissue engineering technologies, such as three-dimensional bioprinting and microfluidic systems, to optimize its delivery and efficacy. These approaches, combined with finely tuned dosage protocols, could facilitate the advancement of personalized regenerative medicine, providing effective solutions for bone repair and regeneration.

## 5. Conclusions

This study investigated the impact of dexamethasone on stem cell spheroids, focusing on their ability to preserve structural integrity, enhance cell viability, and promote osteogenic differentiation. The findings indicated that dexamethasone facilitated cellular survival and significantly increased the expression of RUNX2 and COL1A1 in stem cell spheroids. The incorporation of stem cells with dexamethasone presents a promising strategy for regenerative medicine and therapeutic applications. Future research should concentrate on optimizing dosage levels, developing efficient delivery systems, and assessing the long-term outcomes of these treatments.

**Author Contributions:** Conceptualization, J.-H.K., H.L., H.-J.L., and J.-B.P.; formal analysis, J.-H.K., H.L., H.-J.L., and J.-B.P.; writing—original draft preparation, J.-H.K., H.L., H.-J.L., and J.-B.P.; and writing—reviewing and editing, J.-H.K., H.L., H.-J.L., and J.-B.P. All authors have read and agreed to the published version of the manuscript.

**Funding:** This study was financed by a National Research Foundation of Korea (NRF) grant awarded by the Korean government (MSIT) (No. RS-2023-00252568).

**Institutional Review Board Statement:** The Institutional Review Board of Seoul St. Mary's Hospital, College of Medicine, The Catholic University of Korea, examined and approved the current study protocol (IRB code: KC22SISI0513, date: 22 August 2022).

**Informed Consent Statement:** The individual granted informed consent.

**Data Availability Statement:** The original contributions presented in this study are included in the article; further inquiries can be directed to the corresponding author.

**Acknowledgments:** Parts of this paper was submitted as an abstract at the 111th Annual Meeting of the American Academy of Periodontology.

**Conflicts of Interest:** Regarding this investigation, the authors have no competing interests.

## References

1. Xian, B.; Luo, Z.; Li, K.; Li, K.; Tang, M.; Yang, R.; Lu, S.; Zhang, H.; Ge, J. Dexamethasone Provides Effective Immunosuppression for Improved Survival of Retinal Organoids after Epiretinal Transplantation. *Stem Cells Int.* **2019**, 2019, 7148032. [\[CrossRef\]](#)
2. Ashour, S.H.; Mudalal, M.; Al-Arooomi, O.A.; Al-Attab, R.; Li, W.; Yin, L. The Effects of Injectable Platelet-Rich Fibrin and Advanced-Platelet Rich Fibrin on Gingival Fibroblast Cell Vitality, Proliferation, Differentiation. *Tissue Eng. Regen. Med.* **2023**, 20, 1161–1172. [\[CrossRef\]](#)
3. Rawat, S.; Dadhwal, V.; Mohanty, S. Dexamethasone priming enhances stemness and immunomodulatory property of tissue-specific human mesenchymal stem cells. *BMC Dev. Biol.* **2021**, 21, 16. [\[CrossRef\]](#)
4. Della Bella, E.; Buetti-Dinh, A.; Licandro, G.; Ahmad, P.; Basoli, V.; Alini, M.; Stoddart, M.J. Dexamethasone Induces Changes in Osteogenic Differentiation of Human Mesenchymal Stromal Cells via SOX9 and PPARG, but Not RUNX2. *Int. J. Mol. Sci.* **2021**, 22, 4785. [\[CrossRef\]](#)
5. Chen, Y.; Chen, S.; Kawazoe, N.; Chen, G. Promoted Angiogenesis and Osteogenesis by Dexamethasone-loaded Calcium Phosphate Nanoparticles/Collagen Composite Scaffolds with Microgroove Networks. *Sci. Rep.* **2018**, 8, 14143. [\[CrossRef\]](#)
6. Toledano-Osorio, M.; de Luna-Bertos, E.; Toledano, M.; Manzano-Moreno, F.J.; Costela-Ruiz, V.; Ruiz, C.; Gil, J.; Osorio, R. Dexamethasone and doxycycline functionalized nanoparticles enhance osteogenic properties of titanium surfaces. *Dent. Mater.* **2023**, 39, 616–623. [\[CrossRef\]](#)
7. Park, J.B.; Kim, I.; Lee, W.; Kim, H. Evaluation of the regenerative capacity of stem cells combined with bone graft material and collagen matrix using a rabbit calvarial defect model. *J. Periodontal Implant Sci.* **2023**, 53, 467–477. [\[CrossRef\]](#)
8. Khaled, M.M.; Ibrahim, A.M.; Abdelgalil, A.I.; El-Saied, M.A.; El-Bably, S.H. Regenerative Strategies in Treatment of Peripheral Nerve Injuries in Different Animal Models. *Tissue Eng. Regen. Med.* **2023**, 20, 839–877. [\[CrossRef\]](#)
9. Leypold, T.; Herbsthofer, A.; Craveiro, R.B.; Wolf, M.; Beier, J.P.; Ruhl, T. Effects of cannabinoid receptor activation on Porphyromonas gingivalis lipopolysaccharide stimulation in human periodontal ligament stem cells in vitro. *J. Periodontal Implant Sci.* **2024**, 55, 18. [\[CrossRef\]](#)
10. Kang, S.H.; Park, J.B.; Kim, I.; Lee, W.; Kim, H. Assessment of stem cell viability in the initial healing period in rabbits with a cranial bone defect according to the type and form of scaffold. *J. Periodontal Implant Sci.* **2019**, 49, 258–267. [\[CrossRef\]](#)
11. Arai, Y.; Lee, S.H. MMP13-Overexpressing Mesenchymal Stem Cells Enhance Bone Tissue Formation in the Presence of Collagen Hydrogel. *Tissue Eng. Regen. Med.* **2023**, 20, 461–471. [\[CrossRef\]](#)
12. Zhou, A.K.; Jou, E.; Lu, V.; Zhang, J.; Chabra, S.; Abishek, J.; Wong, E.; Zeng, X.; Guo, B. Using Pre-Clinical Studies to Explore the Potential Clinical Uses of Exosomes Secreted from Induced Pluripotent Stem Cell-Derived Mesenchymal Stem cells. *Tissue Eng. Regen. Med.* **2023**, 20, 793–809. [\[CrossRef\]](#)
13. Suhandi, C.; Mohammed, A.F.A.; Wilar, G.; El-Rayyes, A.; Wathoni, N. Effectiveness of Mesenchymal Stem Cell Secretome on Wound Healing: A Systematic Review and Meta-analysis. *Tissue Eng. Regen. Med.* **2023**, 20, 1053–1062. [\[CrossRef\]](#) [\[PubMed\]](#)
14. Kang, Y.; Na, J.; Karima, G.; Amirthalingam, S.; Hwang, N.S.; Kim, H.D. Mesenchymal Stem Cell Spheroids: A Promising Tool for Vascularized Tissue Regeneration. *Tissue Eng. Regen. Med.* **2024**, 21, 673–693. [\[CrossRef\]](#)
15. Lee, K.; Ko, E.; Park, Y. Adipose Tissue-Derived Mesenchymal Stem Cell Inhibits Osteoclast Differentiation through Tumor Necrosis Factor Stimulated Gene-6. *Tissue Eng. Regen. Med.* **2024**, 21, 587–594. [\[CrossRef\]](#) [\[PubMed\]](#)
16. Wolff, A.; Frank, M.; Staehlke, S.; Springer, A.; Hahn, O.; Meyer, J.; Peters, K. 3D Spheroid Cultivation Alters the Extent and Progression of Osteogenic Differentiation of Mesenchymal Stem/Stromal Cells Compared to 2D Cultivation. *Biomedicines* **2023**, 11, 1049. [\[CrossRef\]](#)
17. Cho, C.S.; Jo, I. Bone Morphogenic Protein-2-Conjugated Three-Dimensional-Printed Poly (L-Lactic Acid) (PLLA) Scaffold is likely Promising as an Effective Bone Substitute. *Tissue Eng. Regen. Med.* **2023**, 20, 155–156. [\[CrossRef\]](#) [\[PubMed\]](#)
18. Kim, D.Y.; Park, G.; Hong, H.S.; Kim, S.; Son, Y. Platelet-Derived Growth Factor-BB Priming Enhances Vasculogenic Capacity of Bone Marrow-Derived Endothelial Precursor Like Cells. *Tissue Eng. Regen. Med.* **2023**, 20, 695–704. [\[CrossRef\]](#)
19. Dobson, L.K.; Zeitouni, S.; McNeill, E.P.; Bearden, R.N.; Gregory, C.A.; Saunders, W.B. Canine Mesenchymal Stromal Cell-Mediated Bone Regeneration is Enhanced in the Presence of Sub-Therapeutic Concentrations of BMP-2 in a Murine Calvarial Defect Model. *Front. Bioeng. Biotechnol.* **2021**, 9, 764703. [\[CrossRef\]](#)

20. Nakayama, Y.; Ogihara-Takeda, M.; Saito, Y.; Yamaguchi, A.; Ogata, Y. Early wound healing at 1 week postoperatively in periodontal tissue regeneration therapy: Enamel matrix derivative versus recombinant human fibroblast growth factor. *J. Periodontal Implant Sci.* **2024**, *54*, 405–418. [\[CrossRef\]](#)
21. Michelo, C.M.; Fasse, E.; van Cranenbroek, B.; Linda, K.; van der Meer, A.; Abdelrazik, H.; Joosten, I. Added effects of dexamethasone and mesenchymal stem cells on early Natural Killer cell activation. *Transpl. Immunol.* **2016**, *37*, 1–9. [\[CrossRef\]](#)
22. Rivera-Cruz, C.M.; Shearer, J.J.; Figueiredo Neto, M.; Figueiredo, M.L. The Immunomodulatory Effects of Mesenchymal Stem Cell Polarization within the Tumor Microenvironment Niche. *Stem Cells Int.* **2017**, *2017*, 4015039. [\[CrossRef\]](#) [\[PubMed\]](#)
23. Wang, H.; Pang, B.; Li, Y.; Zhu, D.; Pang, T.; Liu, Y. Dexamethasone has variable effects on mesenchymal stromal cells. *Cytotherapy* **2012**, *14*, 423–430. [\[CrossRef\]](#)
24. Lee, H.; Hwa, S.; Cho, S.; Kim, J.H.; Song, H.J.; Ko, Y.; Park, J.B. Impact of Polydeoxyribonucleotides on the Morphology, Viability, and Osteogenic Differentiation of Gingiva-Derived Stem Cell Spheroids. *Medicina* **2024**, *60*, 1610. [\[CrossRef\]](#) [\[PubMed\]](#)
25. Daniyal, M.; Liu, Y.; Yang, Y.; Xiao, F.; Fan, J.; Yu, H.; Qiu, Y.; Liu, B.; Wang, W.; Yuhui, Q. Anti-gastric cancer activity and mechanism of natural compound “Heilaohulignan C” isolated from *Kadsura coccinea*. *Phytother. Res.* **2021**, *35*, 3977–3987. [\[CrossRef\]](#)
26. Byeon, S.M.; Bae, T.S.; Lee, M.H.; Ahn, S.G. Guided bone regeneration of calcium phosphate-coated and strontium ranelate-doped titanium mesh in a rat calvarial defect model. *J. Periodontal Implant Sci.* **2024**, *54*, 336–348. [\[CrossRef\]](#) [\[PubMed\]](#)
27. Dong, K.; Zhou, W.J.; Liu, Z.H. Metformin enhances the osteogenic activity of rat bone marrow mesenchymal stem cells by inhibiting oxidative stress induced by diabetes mellitus: An in vitro and in vivo study. *J. Periodontal Implant Sci.* **2023**, *53*, 54–68. [\[CrossRef\]](#)
28. Lee, H.; Park, J.B. Dimethyl Sulfoxide Leads to Decreased Osteogenic Differentiation of Stem Cells Derived from Gingiva via Runx2 and Collagen I Expression. *Eur. J. Dent.* **2019**, *13*, 131–136. [\[CrossRef\]](#)
29. Hwang, J.; Lee, J.H.; Kim, Y.J.; Hwang, I.; Kim, Y.Y.; Kim, H.S.; Park, D.Y. Highly accurate measurement of the relative abundance of oral pathogenic bacteria using colony-forming unit-based qPCR. *J. Periodontal Implant Sci.* **2024**, *54*, 444–457. [\[CrossRef\]](#)
30. Yuasa, M.; Yamada, T.; Taniyama, T.; Masaoka, T.; Xuetao, W.; Yoshii, T.; Horie, M.; Yasuda, H.; Uemura, T.; Okawa, A.; et al. Dexamethasone enhances osteogenic differentiation of bone marrow- and muscle-derived stromal cells and augments ectopic bone formation induced by bone morphogenetic protein-2. *PLoS ONE* **2015**, *10*, e0116462. [\[CrossRef\]](#)
31. Tangtrongsup, S.; Kisiday, J.D. Effects of Dexamethasone Concentration and Timing of Exposure on Chondrogenesis of Equine Bone Marrow-Derived Mesenchymal Stem Cells. *Cartilage* **2016**, *7*, 92–103. [\[CrossRef\]](#) [\[PubMed\]](#)
32. Ma, L.; Feng, X.; Wang, K.; Song, Y.; Luo, R.; Yang, C. Dexamethasone promotes mesenchymal stem cell apoptosis and inhibits osteogenesis by disrupting mitochondrial dynamics. *FEBS Open Bio.* **2020**, *10*, 211–220. [\[CrossRef\]](#)
33. Abu-Absi, S.F.; Hu, W.S.; Hansen, L.K. Dexamethasone effects on rat hepatocyte spheroid formation and function. *Tissue Eng.* **2005**, *11*, 415–426. [\[CrossRef\]](#)
34. Meesuk, L.; Suwanprateeb, J.; Thammarakcharoen, F.; Tantrawatpan, C.; Kheolamai, P.; Palang, I.; Tantikanlayaporn, D.; Manochantr, S. Osteogenic differentiation and proliferation potentials of human bone marrow and umbilical cord-derived mesenchymal stem cells on the 3D-printed hydroxyapatite scaffolds. *Sci. Rep.* **2022**, *12*, 19509. [\[CrossRef\]](#)
35. Amini, A.R.; Laurencin, C.T.; Nukavarapu, S.P. Bone tissue engineering: Recent advances and challenges. *Crit. Rev. Biomed. Eng.* **2012**, *40*, 363–408. [\[CrossRef\]](#)
36. Chen, R.; Wang, M.; Qi, Q.; Tang, Y.; Guo, Z.; Wu, S.; Li, Q. Sequential anti-inflammatory and osteogenic effects of a dual drug delivery scaffold loaded with parthenolide and naringin in periodontitis. *J. Periodontal Implant Sci.* **2023**, *53*, 20–37. [\[CrossRef\]](#)
37. Feng, J.; Meng, Z. Insulin growth factor-1 promotes the proliferation and osteogenic differentiation of bone marrow mesenchymal stem cells through the Wnt/ $\beta$ -catenin pathway. *Exp. Ther. Med.* **2021**, *22*, 891. [\[CrossRef\]](#)
38. Devos, H.; Zoidakis, J.; Roubelakis, M.G.; Latosinska, A.; Vlahou, A. Reviewing the Regulators of COL1A1. *Int. J. Mol. Sci.* **2023**, *24*, 10004. [\[CrossRef\]](#)
39. Wu, H.; Liao, X.; Wu, T.; Xie, B.; Ding, S.; Chen, Y.; Song, L.; Wei, B. Mechanism of MiR-145a-3p/Runx2 pathway in dexamethasone impairment of MC3T3-E1 osteogenic capacity in mice. *PLoS ONE* **2024**, *19*, e0309951. [\[CrossRef\]](#) [\[PubMed\]](#)
40. De Pace, R.; Iaquina, M.R.; Benkhalqui, A.; D’Agostino, A.; Trevisiol, L.; Nocini, R.; Mazziotta, C.; Rotondo, J.C.; Bononi, I.; Tognon, M.; et al. Revolutionizing bone healing: The role of 3D models. *Cell Regen.* **2025**, *14*, 7. [\[CrossRef\]](#) [\[PubMed\]](#)
41. Murphy, K.C.; Hoch, A.I.; Harvestine, J.N.; Zhou, D.; Leach, J.K. Mesenchymal Stem Cell Spheroids Retain Osteogenic Phenotype Through  $\alpha 2 \beta 1$  Signaling. *Stem Cells Transl. Med.* **2016**, *5*, 1229–1237. [\[CrossRef\]](#)
42. Liu, X.; Astudillo Potes, M.D.; Dashtdar, B.; Schreiber, A.C.; Tilton, M.; Li, L.; Elder, B.D.; Lu, L. 3D Stem Cell Spheroids with 2D Hetero-Nanostructures for In Vivo Osteogenic and Immunologic Modulated Bone Repair. *Adv. Healthc. Mater.* **2024**, *13*, e2303772. [\[CrossRef\]](#) [\[PubMed\]](#)
43. Melnik, D.; Sahana, J.; Corydon, T.J.; Kopp, S.; Nassef, M.Z.; Wehland, M.; Infanger, M.; Grimm, D.; Krüger, M. Dexamethasone Inhibits Spheroid Formation of Thyroid Cancer Cells Exposed to Simulated Microgravity. *Cells* **2020**, *9*, 367. [\[CrossRef\]](#) [\[PubMed\]](#)

44. Okamura, H.; Yoshida, K.; Yang, D.; Haneji, T. Protein phosphatase 2A C $\alpha$  regulates osteoblast differentiation and the expressions of bone sialoprotein and osteocalcin via osterix transcription factor. *J. Cell. Physiol.* **2013**, *228*, 1031–1037. [[CrossRef](#)]
45. Getova, V.E.; Orozco-García, E.; Palmers, S.; Krenning, G.; Narvaez-Sanchez, R.; Harmsen, M.C. Extracellular Vesicles from Adipose Tissue-Derived Stromal Cells Stimulate Angiogenesis in a Scaffold-Dependent Fashion. *Tissue Eng. Regen. Med.* **2024**, *21*, 881–895. [[CrossRef](#)]

**Disclaimer/Publisher’s Note:** The statements, opinions and data contained in all publications are solely those of the individual author(s) and contributor(s) and not of MDPI and/or the editor(s). MDPI and/or the editor(s) disclaim responsibility for any injury to people or property resulting from any ideas, methods, instructions or products referred to in the content.